26th EPS Conf. on Contr. Fusion and Plasma Physics, Maastricht, 14 - 18 June 1999 ECA Vol.23J (1999) 1449 - 1452

STUDIES ON THE SCALING OF H-MODE PEDESTAL WIDTH IN THE ITER MULTI-MACHINE PEDESTAL DATABASE

M. Sugihara[1], Yu. Igitkhanov[1], G. Janeschitz[1], T. Hatae[2], L. Horton[3], A. Hubbard[4], Y. Kamada[2], J. Lingertat[3], T. Osborne[5], W. Suttrop[6] and ITER H-mode Edge Pedestal Expert Group

[1] *ITER Joint Central Team, Joint Work Site, D-85748 Garching, Germany*
[2] *JAERI, Naka Fusion Research Establishment, Ibaraki-ken, 311-01 Japan*
[3] *JET Joint Undertaking, Abingdon Oxon., OX14 3EA, UK*
[4] *Plasma Fusion Centre, MIT, Cambridge, MA 01239, USA*
[5] *General Atomics, P.O. Box 85608, San Diego, CA 92186-5608 USA*
[6] *Max-Planck-Institut für Plasmaphysik, EURATOM Assoc., D-85748 Garching, Germany*

1. Introduction

Energy confinement during H-mode in Tokamaks strongly depends on the temperature at the top of the H-mode pedestal [1]. This pedestal temperature is determined by the gradient and the width of the pedestal edge. In the case of the Type-I ELMy regime, which is assumed for pulsed operation in ITER, it is widely observed that the pressure gradient is close to the ideal ballooning stability limit. Thus, the discharge parameter and machine size dependence of the pedestal width is of primary importance for predicting the pedestal temperature in ITER.

The ITER multi-machine pedestal database activity has been started to identify the overall features of the pedestal region for the various discharge modes including the LH transition, Type I and Type III ELMs, the ELM-free and EDA (Enhanced D_α) phases. For these regimes, the pedestal data (mainly scalar data and limited data for profiles from some machines) from major divertor Tokamaks, ASDEX-U(AUG), C-MOD, DIII-D, JET and JT-60U, are archived in the database. Although the data archive is still on-going, this paper presents an initial study on the pedestal width/height during the ELM-free, EDA and Type I ELMy phases based on the presently available data.

So far, the width studies have been limited to one machine [2-6] or at most to a comparison between two machines (C-MOD and DIII-D [7]). Studies show, however, that the parameter dependence of the pedestal width is rather different from machine to machine, e.g., some machines observe ion poloidal Larmor radius dependence when considering thermal or fast ions [8, 9], while such dependence is not observed in some machines [6]. Universal scaling is still difficult to derive. Another limitation of the database is that direct comparison of the width is not possible in many machines due to diagnostic limitations. Thus, in this paper, we mainly examine the pedestal pressure in terms of several candidate width scalings such as poloidal Larmor radius and other theoretical models assuming that the pressure gradient is determined by the ideal ballooning stability limit.

We will also propose one possible interpretation of the divergent observations of the width based on turbulence suppression by a combination of the electric and magnetic field shear. Some examinations on this interpretation on the database are also presented.

2. Examination on pedestal height

Several machines observe the ion poloidal Larmor radius dependence for the pedestal width and a majority of the machines observe the critical pressure gradient which is close to the ideal ballooning limit. Thus, as an initial choice of the scaling parameters for the pedestal height, we will employ $(dp/dr)_c \rho_{pol}$, where $(dp/dr)_c = \frac{1}{2\mu_0 R}\left(\frac{R}{a}\bar{B}_p\right)^2 \frac{2}{1+\kappa^2}$ is the critical pressure gradient for the ideal ballooning mode, ρ_{pol} is the ion poloidal Larmor radius measured at the pedestal temperature and $\bar{B}_p$ is the average poloidal field in cylinder approximation with elliptic cross section. Total pressure is evaluated by twice the electron pressure, except for JT-60U, in which ion pedestal temperature is routinely measured by CXR. In C-MOD and JT-60U, density and temperature at 95 % flux surface are used for the pedestal values assuming that they are very

close to the pedestal quantities. This may underestimate the pedestal temperature (T_{ped}) in C-MOD, which can have wider pedestals. In C-MOD, the pedestal density is assumed to be 2/3 of the line average density [2]. In DIII-D and AUG, pedestal values are evaluated by tanh fitting, whereas, in JET, they are evaluated by linear fitting. Several fitting exercises show that the pedestal top values by both fitting methods are very similar. Each machine has generally good correlation with this scaling parameter and the summary results are shown in Fig. 1, where data from all machines for various operation regimes are plotted together : Type-I ELMy (AUG, DIII-D, JET), ELM-free (C-MOD, JT-60U) and EDA (C-MOD). Generally good correlation can be seen for each machine, though each machine has a very different proportional coefficient and there are some scatter and some systematic deviations. It is also seen that the ELM-free data (assuming that EDA are similar to ELM-free) have lower pedestal pressure due mainly to narrower width. Possible underestimates of T_{ped} in C-MOD may partly explain why C-MOD points tend to lie below the others. DIII-D data have a similar tendency, though they are in a different operation regime with fairly steep gradient and narrow width, which are supposed to be in the second stability regime. Other important dependences to be examined are (i) the effect of plasma shaping (triangularity δ), (ii) difference by different operation regime (ELM-free vs. ELMy or second stability), (iii) size dependence. We first examine the effect of δ using the results from series of discharges with changing δ in JT-60U [10]. From these experiments, enhancement factor for the critical pressure gradient by δ at 95 % flux surface, $g(\delta)$ can be expressed as $g(\delta) = 1 + 9.3\delta^{3.4}$. This is consistent with DIII-D experimental results, in which the pedestal pressure with two different separatrix δ are compared. With the enhancement factor $g(\delta)$, the pedestal pressure data are re-summarised by $(dp/dr)_c \rho_{pol} g(\delta)$, which is shown in Fig. 2 Although the correlation still remains generally good by introducing the triangularity effect, no significant improvement for the scatter of data in each machine can be seen. In this figure, JET and JT-60U have similar size and plasma shape effect is already included, so that the remaining difference between two machines could be that of operation regime (ELM-free for JT-60U and ELMy for JET). In fact, if we make proper correction based on the comparison between ELM-free and ELMy in JT-60U [5], i.e., pedestal width increases by a factor 2-3 in ELMy phase, JT-60U data become fairly close to the JET data. DIII-D data are now somewhat deviating from JET line and C-MOD data are clearly shifting to the right due to its high δ. The figure also indicates that the pedestal top values in DIII-D may scale not so much differently regardless of the operation regime (1st and 2nd stability regime), since DIII-D has almost the same size as AUG and shaping difference is already included in the figure.

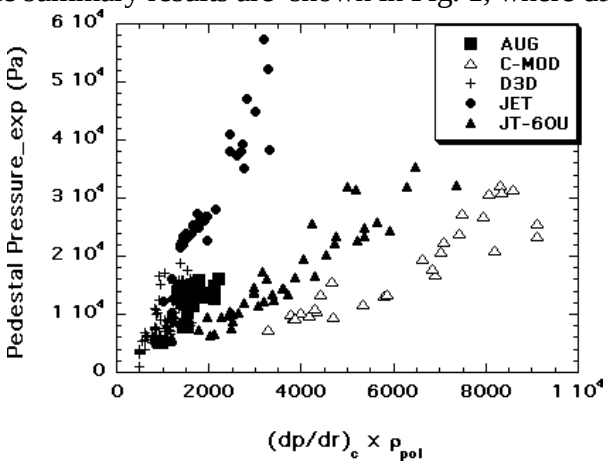

Fig. 1 Experimental pedestal pressure for all machines as summarised by a chosen scaling of critical pressure gradient times poloidal Larmor radius.

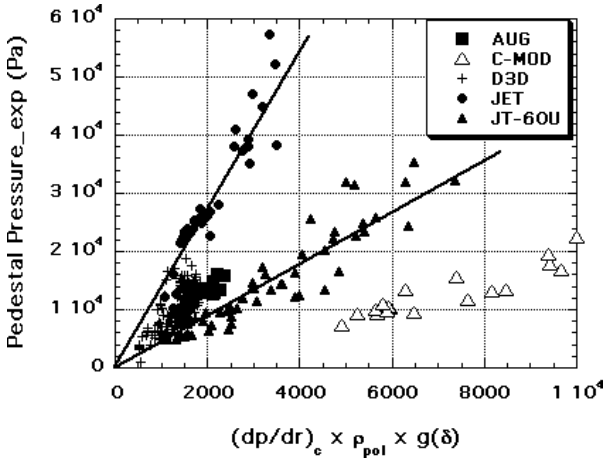

Fig. 2 Experimental pedestal pressure for all machines with inclusion of triangularity effect.

Another indication for size effect could be seen from the comparison between C-MOD vs. JT-60U, and JET vs. AUG, since they are in the same discharge regime, respectively. However, further detailed investigations on these effects and derivation of the scaling need more systematic experiments in each machine and comparisons of these data, which is to be performed in future.

3. Examinations of various theoretical models for pedestal width/height

In this section, we will briefly examine several theoretical models proposed so far by using the ITER pedestal database. It is proposed that ρ_{pol} (or banana width; ρ_{ban}) scaling with fast ion energy can explain the JET experimental observation that the T_{ped} dependence of the width is weaker than that of the Larmor radius (square root of T_{ped}) for fixed plasma current and toroidal field discharges [9]. Although, in JET, the experimentally inferred width of 5-7 cm are exactly in the range of ρ_{ban} evaluated with the injected beam energy E_b of 120 keV, data from other machines in the database show clear contradiction, especially for small machines, i.e., (0.5-1) E_b for JT-60U, (0.2-0.3) E_b for AUG, (0.03-0.07) E_b for DIII-D are expected to reproduce the experimental width by ρ_{ban}. In addition, no fast ions are expected for the ICRF heating in C-MOD. Moreover, this approach cannot explain the experimental fact that the pedestal width during the ELM-free phase is much narrower than that during ELMy phase, while no substantial difference in the fast ion energy and population will be expected during both phases.

Among several theoretical models, the mode structure of the edge drift ballooning mode with the poloidal rotation provided by the Reynolds stress predicts the pedestal width as $\rho_{pol}^{2/3} a^{1/3}$, with which DIII-D data are also found to fit well [3]. Although with this width scaling the pedestal pressure in the database can be fitted similarly well as in Fig. 1, Reynolds stress is actually expected to be too weak to suppress the turbulence. Many of the remaining theoretical predictions based on the suppression of micro turbulence suggest that the width should scale as ρ_{tor} instead of ρ_{pol}. Thus, in these models, plasma current dependence, which is observed in many machines, must be appropriately explained.

4. Width scaling with ρ_{tor} and its current dependence

In this section, we propose a new width scaling with ρ_{tor}. The underlying physics is that the edge transport barrier is formed where the turbulence growth rate is balanced by a stabilizing ExB shearing rate, which is dominantly produced by a steep pressure gradient during a well developed H-mode phase. The magnetic shear S also plays an essential role under this condition through the fact that the critical pressure gradient for the ideal ballooning mode is increased and the turbulence growth rate is decreased with increasing the shear. Here let us employ very simplified expressions for both turbulence growth rate γ_s and stabilizing ExB shearing rate γ_{ExB} arising from the critical pressure gradient. The stabilizing condition can be written as $\gamma_{ExB} \geq \gamma_s$. Assuming that the dominant contribution to the radial electric field is the pressure gradient, which is determined by the ideal ballooning mode, γ_{ExB} is expressed as in Eq. (1). Here, c_s and x_0 are the sound velocity and the width scale length, respectively. We have assumed a simplified $S-\alpha$ diagram for the ballooning stability. For the turbulence growth rate, we will assume a simplified expression for the gyro-Bohm type transport including the stabilising effect due to the magnetic shear as in Eq. (2), where $\kappa_\perp \rho_{tor} \approx O(1)$ is assumed. From Eqs (1),(2), the pedestal width Δ scales as Eq. (3). Pedestal pressure evaluated with this width is very consistent with the scaling derived in JET recently [11]. Although this is derived by very simplified assumptions, many experimental features seem qualitatively consistent with this expression. For instance, with increasing plasma current I_p, the edge shear decreases, so that the width scales inversely with I_p (ion poloidal-Larmor-radius like dependence). The shear increases with δ, which increases the width as observed in C-MOD [7]. The ion mass dependence can be retained through the toroidal Larmor radius. Examinations of this scaling with C-MOD and JET data show that it can

$$\gamma_{ExB} \approx S \frac{\rho_{tor} c_s}{x_0^2} \quad (1)$$

$$\gamma_s \approx \chi_{GB} \kappa_\perp^2 \approx \rho_{tor} c_s \frac{\rho_{tor}}{x_0} \kappa_\perp^2 \frac{1}{S} \approx \frac{c_s}{x_0} \frac{1}{S} \quad (2)$$

$$\Delta \propto \rho_{tor} S^2 \quad (3)$$

reproduce the data at least similarly well as the scaling based on ρ_{pol}. Fig. 3 shows the T_{ped} with changing the pedestal density n_{ped} for fixed I_P(=2.5 MA) and B_T(=2.3 T) in JET [4] (closed squares). Dotted and dashed lines are expected T_{ped}, when the width are constant and poloidal Larmor radius like, respectively. Open circles show the expected T_{ped} when the width is evaluated by Eq. (3) using the experimental shear values. Although the evaluated points show some scatter due mainly to the scatter of shears calculated by EFIT code, they reproduce the experimental tendency reasonably well. This is realised by the decrease of shear with decreasing n_{ped} and increasing T_{ped}. The most likely mechanism of this systematic decrease of shear is the effect of bootstrap current. Larger bootstrap current is expected to flow when n_{ped} decreases, since collisionality strongly decreases. This larger bootstrap current decreases the edge shear, which makes the deviation of the pedestal pressure from Larmor radius dependence of the width. This bootstrap current may not directly influence the shear value in the EFIT calculation. However, it can modify the equilibrium even for fixed B_T and I_P, which can resultantly modify the shear value. More comprehensive equilibrium code calculation including bootstrap current self-consistently is needed to confirm this mechanism, which is beyond the scope of this paper and deserves future study. DIII-D data in the database are not reproduced reasonably well by this scaling. The reason for this discrepancy is somewhat trivial when we consider that the DIII-D pedestals are in the 2nd stability regime. Then, the relation between critical gradient and shear cannot be expressed as simply proportional to shear, which modifies the shear dependence of Eq. (1) greatly. To derive the width scaling for these regimes, full treatment of the ballooning stability including the effect of bootstrap current is needed. Note that by considering the spatial structure of the shear, a size dependence can be derived, which results in T_{ped}≈3-4 keV for ITER based on an example model profile for shear.

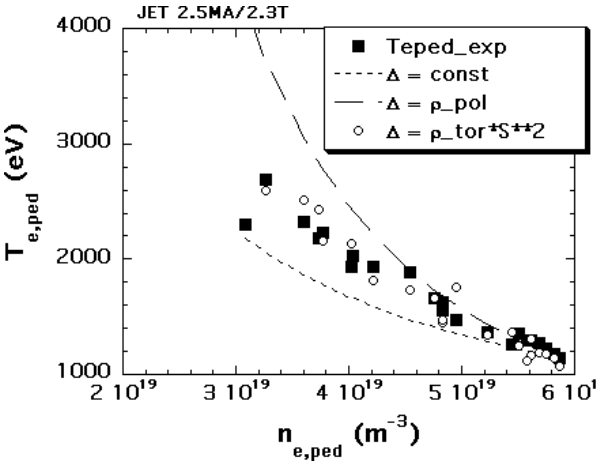

Fig. 3 Experimental pedestal temperature (closed square) for fixed toroidal field and current discharge in JET. Open circles, dotted line and dashed line show expected pedestal temperature by width scaling of Eq. (3), constant width and poloidal Larmor dependent width, respectively.

5. Summary

Examinations of the ITER multi-machine pedestal database show that the pedestal heights during ELM-free, EDA and Type-I ELMy phases have a good correlation with the critical gradient for the ideal ballooning times poloidal Larmor radius, though they are clearly separated depending on the discharge regimes and probably size. Scaling with toroidal Larmor radius and magnetic shear could explain many features of the width experimentally observed, and further investigation is to be done in parallel with more systematic data archiving in the database.

References

[1] G. Janeschitz, et al., 26 th EPS Conf. on Contr. Fusion Plas. Physics, Maastrich, 1999.
[2] A. E. Hubbard, R. L. Boivin, R. S. Granetz, et al., Phys. Plasmas **5** (1998) 1744.
[3] T. H. Osborne, K. H. Burrell, R. J. Groebner, et al., J. Nucl. Mat. **266-269** (1999) 131.
[4] J. Lingertat, V. Bhatnager, G. D. Conway, et al., J. Nucl. Mat. **266-269** (1999) 124.
[5] Y. Kamada, et al., 17th IAEA Fus. Energy Conf. 1998, IAEA-F1-CN-69/CD2/EX9/2.
[6] W. Suttrop, et al., Plasma Phys. Control. Fusion **39** (1997) 2051.
[7] R. S. Granetz, et al., 17th IAEA Fus. Energy Conf., 1998, IAEA-F1-CN-69/EX6/2.
[8] T. Hatae, Y. Kamada, S. Ishida, et al., Plasma Phys. Control. Fusion **40** (1998) 1073.
[9] V. Parail, H. Y. Guo and J. Lingertat, to be published in Nucl. Fusion, 1998.
[10] Y. Kamada, et al., 16th IAEA Fus. Energy Conf., Montreal, 1996, IAEA-CN-64/A1-6.
[11] G. Saibene, L. D. Horton, R. Sartori, et al., submitted to Nucl. Fusion (1999).